NJC

RSC Publishing

PAPER

View Article Online
View Journal | View Issue

Cite this: *New J. Chem.*, 2013, **37**, 3737

Recognition of dihydrogen phosphate ions using the cadmium complex of 2-pyridine-1*H*-imidazo[4,5-*b*]-phenazine: utilization of the mechanism of twisted intramolecular charge transfer, long wavelength emission†

BingBing Shi, YouMing Zhang,* TaiBao Wei, Peng Zhang, Qi Lin and Hong Yao

Received (in Montpellier, France) 31st May 2013,
Accepted 19th August 2013

DOI: 10.1039/c3nj00578j

www.rsc.org/njc

A long wavelength emission fluorescent and colorimetric chemosensor with high selectivity for $H_2PO_4^-$ ions was designed and synthesized according to the twisted intramolecular charge transfer (TICT) mechanism. The sensor bears a 2-pyridine-1*H*-imidazo[4,5-*b*]phenazine and Cd^{2+} metal complex, which showed brilliant fluorescent and colorimetric response for $H_2PO_4^-$ anions in aqueous solution. The detection limit of the sensor towards $H_2PO_4^-$ is 2.8×10^{-6} M, and other anions, including F^-, Cl^-, Br^-, I^-, AcO^-, HSO_4^-, ClO_4^- and CN^-, had nearly no influence on the probing behavior. The test strips based on the 2-pyridine-1*H*-imidazo[4,5-*b*]phenazine and Cd^{2+} metal complex (S_2–Cd) were fabricated, which could act as convenient and efficient $H_2PO_4^-$ test kits.

1. Introduction

Among various anions, phosphate ions are of particular interest as they are key substrates for many biochemical reactions and are main components of biomolecules.[1] Recently, numerous metal-based receptors, particularly Zn(II) complexes, have been reported for fluorescent sensing of phosphate ions.[2–5] However, due to fluorescence quenching, the dependence on organic solvents or, more specifically, the interference from other anions, there are still major challenges to be overcome in developing highly selective chemosensors for dihydrogen phosphate, and as required by biologists and medical experts, long wavelength emission fluorescent chemosensors are welcome since the signal could easily penetrate the body tissue to facilitate detection and reduce damage.[6–9] In contrast to the zinc-based complexes for the recognition of the dihydrogen phosphate, cadmium-based receptors have seldom been reported.

On the other hand, various fluorescent chemosensors for $H_2PO_4^-$ have been described recently owing to their high selectivity and low background disturbance. In addition to the frequently used fluorescence signaling mechanisms of photoinduced electron transfer (PET) and intramolecular charge transfer (ICT), the concept of twisted intramolecular charge transfer (TICT),[10] proposed by Lippert and co-workers, has seldom been utilized, possibly due to the difficulty in controlling two crucial factors, the degree of the electron transfer and the change in molecular geometry. Correspondingly, the TICT-based fluorescent chemosensors are still very scarce, although in principle, the well-designed ones should show very good performance.

Furthermore, phenazine derivatives have been synthesized and have been used in organic electronics for a long time,[11–14] but they have seldom been used in host–guest chemistry, and there is no report on sensing ions based on its metal complex. Phenazines are ideal platforms for the development of cation, anion, and neutral molecule recognition. Moreover, among the different fluorogenic units, phenazine is very sensitive to conformational change.

Our research group has a longstanding interest in molecular recognition.[15–18] Herein, we have elaborately designed a long wavelength emission, two channel (colorimetric and fluorescent) dihydrogen phosphate chemosensor (S_2–Cd) according to the twisted intramolecular charge transfer (TICT) mechanism based on the 2-pyridine-1*H*-imidazo[4,5-*b*]phenazine and Cd^{2+} complex (S_2, Scheme 1), in which the phenazine group acts as a fluorophore, imidazole and pyridine groups are in the same sensor molecule, to enhance the coordination capacity required

---

Key Laboratory of Eco-Environment-Related Polymer Materials, Ministry of Education of China, Key Laboratory of Polymer Materials of Gansu Province, College of Chemistry and Chemical Engineering, Northwest Normal University, Lanzhou, Gansu, 730070, P. R. China. E-mail: zhangnwnu@126.com; Tel: +086 9317973191

† Electronic supplementary information (ESI) available. See DOI: 10.1039/c3nj00578j

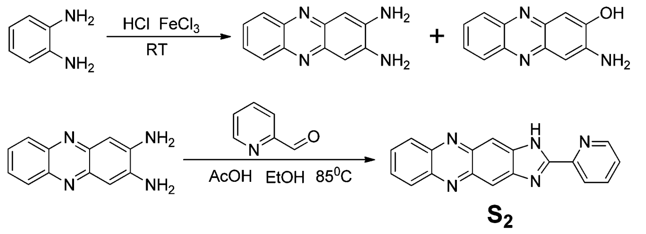

Scheme 1 Synthesis of compound S_2.

to coordinate a cadmium ion. The S_2–Cd sensor showed both colorimetric and fluorescent selectivity for $H_2PO_4^-$ in DMSO–H_2O (8 : 2, v/v) HEPES buffer solutions over other common physiologically important anions. To the best of our knowledge, this is the first time that a long wavelength emission fluorescent cadmium-based chemosensor with high selectivity for $H_2PO_4^-$ was designed.

2. Experimental section

2.1. Materials and physical methods

Fresh double distilled water was used throughout the experiment. All other reagents and solvents were commercially available at analytical grade and were used without further purification. ^{1}H NMR and ^{13}C NMR spectra were recorded on a Mercury-400BB spectrometer at 400 MHz. Chemical shifts are reported in ppm downfield from tetramethylsilane (TMS, δ scale with solvent resonances as internal standards) and UV–vis spectra were recorded on a Shimadzu UV-2550 spectrometer. Photoluminescence spectra were recorded on a Shimadzu RF-5301 fluorescence spectrophotometer. Melting points were measured on an X-4 digital melting-point apparatus (uncorrected). Infrared spectra were recorded on a Digilab FTS-3000 FT-IR spectrophotometer.

2.2. Synthesis of sensor S_2

2,3-Diamino-phenazine was prepared following the reported procedure.[12,13]

Synthesis of compound S_2. 2,3-Diamino-phenazine (0.42 g, 2 mmol), 2-pyridylaldehyde (0.28 g, 2.5 mmol) and a catalytic amount of acetic acid (AcOH) were combined in hot absolute DMF (20 mL). The solution was stirred under reflux conditions for 8 hours; after cooling to room temperature, the brown precipitate was filtrated, washed with hot absolute ethanol three times, then recrystallized with DMF–H_2O to get a brown powdery product S_2 (0.9 mmol) in 45% yield (m.p. > 300 °C), ^{1}H NMR (DMSO-d_6, 400 MHz) δ 13.57 (s 1H, NH), δ 8.88 (d 1H, ArH), 8.59–8.28 (m 2H, ArH) 8.23–8.13 (m 4H, ArH) 7.91–7.88 (m 2H, ArH) 7.67 (m 1H, ArH). ^{13}C-NMR (DMSO-d_6, 150 MHz) δ 158.76, 149.93, 148.84, 147.20, 142.10, 141.78, 140.28, 140.13, 139.71, 137.98, 130.12, 129.75, 129.10, 128.97, 126.49, 123.18, 115.70, 106.88. IR (KBr, cm^{-1}) ν: 3137.21 (NH), 1658.68(C═N). ESI-MS *m*/*z*: $(M + H)^+$ Calcd for $C_{18}H_{11}N_5H$ 298.3; found 298.3. Anal. calcd for $C_{18}H_{11}N_5$: C, 72.73; H, 3.70; N, 23.57%; found C 72.81, H 3.65, N 23.61%.

2.3. General procedure for UV-vis experiments

UV-vis spectroscopy was carried out after the addition of tetrabutylammonium salts in DMSO, while keeping the ligand concentration constant (2.65×10^{-5} M), on a Shimadzu UV-2550 spectrometer. The solutions of the anions were prepared from the tetrabutylammonium salts of $H_2PO_4^-$, F^-, Cl^-, Br^-, I^-, AcO^-, HSO_4^-, ClO_4^-, CN^-, and the Cd^{2+} ion solution was prepared from its perchlorate salt.

2.4. General procedure for fluorescence spectra experiments

Fluorescence spectroscopy was carried out after the addition of tetrabutylammonium salts in DMSO, while keeping the ligand concentration constant (2.65×10^{-5} M), on a Shimadzu RF-5301 fluorescence spectrometer. The excitation wavelength was 400 nm. The solutions of anions were prepared from the tetrabutylammonium salts of $H_2PO_4^-$, F^-, Cl^-, Br^-, I^-, AcO^-, HSO_4^-, ClO_4^-, CN^-, and the Cd^{2+} ion solution was prepared from its perchlorate salt.

2.5. General procedure for ^{1}H NMR experiments

The ^{1}H NMR titration experiment was investigated by addition of increasing concentrations of $Cd(ClO_4)_2$ in DMSO-d_6 to the solution of S_2 (DMSO-d_6) in an NMR tube. Then further experiment was carried out by addition of increasing concentrations of $TBAH_2PO_4$ in DMSO-d_6 solution. The spectra were recorded after mixing and the temperature of the NMR probe was kept constant at 298 K.

3. Results and discussion

To evaluate the binding ability of compound S_2 towards Cd^{2+} ions, we carried out UV-vis and fluorescence experiments in DMSO–H_2O (8 : 2, v/v) buffered with HEPES (pH 7.24, 10 mM) by adding aliquots of Cd^{2+} metal ions as its perchlorate salt. The absorption spectrum of compound S_2 (26.5 μM) in DMSO–H_2O (8 : 2, v/v) HEPES buffer (pH 7.24) solution exhibits two absorption bands at 400 and 264 nm corresponding to phenazine and pyridine, respectively (ESI,† Fig. S1). Upon addition of Cd^{2+} ions (0–27.64 equiv.), the band at 400 nm is red-shifted to 416 nm and the band at 264 nm is red-shifted to 275 nm. Seven isosbestic points are observed at 268, 311, 328, 351, 405, 432 and 475 nm, indicating formation of the S_2–Cd complex (Fig. 1). In the fluorescence spectrum, the emission of S_2 appeared at the maximum emission wavelength was 540 nm in DMSO–H_2O (8 : 2, v/v) HEPES buffer (pH 7.24) solution when excited at λ_{ex} = 416 nm (ESI,† Fig. S2). This is due to twisted intramolecular charge transfer (TICT) from pyridine to the phenazine moiety. Upon addition of increasing amounts of Cd^{2+} ions (0–23.24 equiv.) to the solution of S_2 in DMSO–H_2O (8 : 2, v/v) HEPES buffer (pH 7.24), the fluorescence emission band at 540 nm is red-shifted to 600 nm, directly leading to a strong red emission (Fig. 2). This fluorescence emission band shift is attributed to the formation of the S_2–Cd complex due to interaction between Cd^{2+} ions and imidazole nitrogen and the nitrogen atom of the pyridine moiety as a result of which

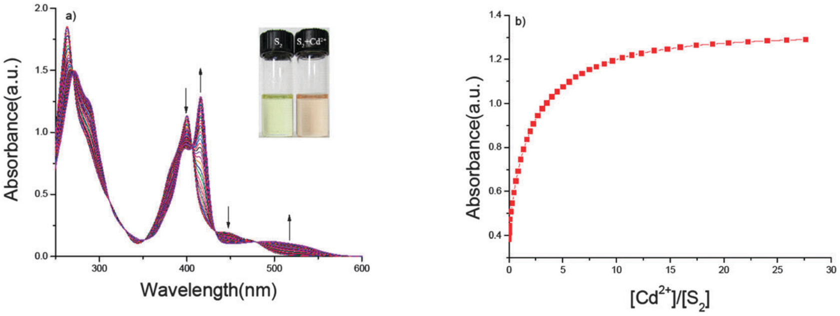

Fig. 1 (a) Absorbance spectra of S_2 (26.5 μM) at different concentrations of Cd^{2+} (0–27.64 equiv.) in DMSO–H_2O (pH = 7.24, v/v = 8 : 2). (b) A plot of absorbance depending on the concentration of Cd^{2+} in the range from 0 to 27.64 equivalents. The detection wavelength was 416 nm.

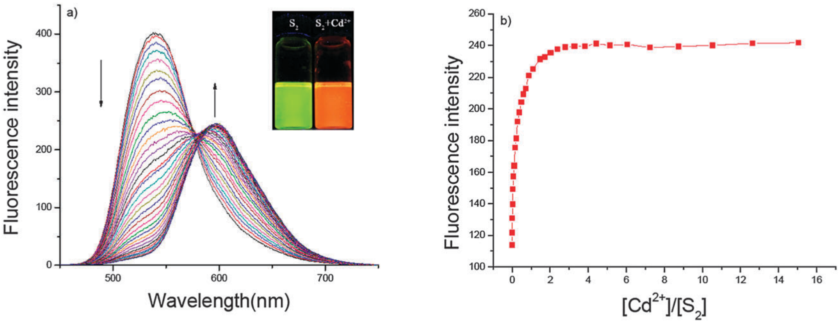

Fig. 2 (a) Fluorescence spectra of S_2 (26.5 μM) at different concentrations of Cd^{2+} in DMSO–H_2O (pH = 7.24, v/v = 8 : 2). (b) A plot of fluorescence intensity depending on the concentration of Cd^{2+} in the range from 0 to 23.14 equivalents. The detection wavelength was 600 nm.

the TICT from the pyridine to the phenazine moiety is suppressed resulting in a fluorescence emission band shift. A Job plot for the binding between S_2 and Cd^{2+} shows a 2 : 1 stoichiometry (Fig. 3), and the association constant of the S_2–Cd complex was determined to be 5.5×10^6 M^{-2} (ESI,† Fig. S3). The 2 : 1 (S_2 : Cd^{2+}) stoichiometry was further confirmed by the ESI-MS spectrum of the S_2–Cd complex where a molecular ion peak at 705.3 was observed, which corresponds to the $[S_2\text{–Cd–H}]^+$ complex (ESI,† Fig. S6).

The recognition profiles of the chemosensor S_2–Cd (15 equiv.) towards various anions, $H_2PO_4^-$, F^-, Cl^-, Br^-, I^-, AcO^-, HSO_4^-, ClO_4^-, CN^-, were primarily investigated by UV-vis spectroscopy and fluorescence spectroscopy in DMSO–H_2O (8 : 2, v/v) HEPES buffer (pH 7.24). When 40 equivalents of $H_2PO_4^-$ were added to the DMSO–H_2O (8 : 2, v/v) HEPES buffer (pH 7.24) solutions of the sensor S_2–Cd (15 equiv.), S_2–Cd responded with a dramatic color change, from pink to yellow. The apparent color change from pink to yellow could be distinguished by the naked eye. The absorption spectrum of the sensor S_2–Cd (15 equiv.) in DMSO–H_2O (8 : 2, v/v) HEPES buffer (pH 7.24) solution exhibits two absorption bands at 416 and 275 nm. When 40 equivalents of $H_2PO_4^-$ were added to the DMSO–H_2O (8 : 2, v/v) HEPES buffer (pH 7.24) solution of the sensor S_2–Cd (15 equiv.), the band at 416 nm is blue-shifted to 400 nm and the band at 275 nm is blue-shifted to 264 nm (Fig. 4). To validate the selectivity of the sensor S_2–Cd (15 equiv.), the same tests were applied using F^-, Cl^-, Br^-, I^-, AcO^-, HSO_4^-, ClO_4^-, CN^- anions, and these anions induced little changes in the UV-vis spectrum of the sensor (Fig. 5). Meanwhile, the fluorescent measurements for the sensor S_2–Cd (15 equiv.) were performed in DMSO–H_2O (8 : 2, v/v) HEPES buffer (pH 7.26) solution. As shown in Fig. 6, in the fluorescence spectrum, the emission of S_2–Cd (15 equiv.) appeared at the maximum emission wavelength was 600 nm in DMSO–H_2O (8 : 2, v/v) HEPES buffer (pH 7.24) solution when excited at λ_{ex} = 400 nm. When 40 equivalents of $H_2PO_4^-$ were added to the DMSO–H_2O (8 : 2, v/v) HEPES buffer (pH 7.24) solutions of the sensor S_2–Cd (15 equiv.), the fluorescence emission band at 600 nm is blue-shifted to 540 nm. The apparent color change from red to yellow could be distinguished by the naked eye. To validate the selectivity of the

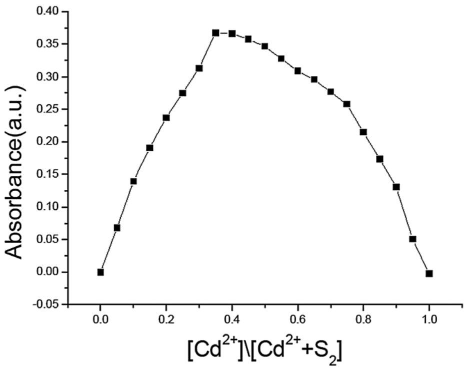

Fig. 3 Job's plot examined between Cd^{2+} and S_2, indicating the 2 : 1 stoichiometry for S_2–Cd clearly.

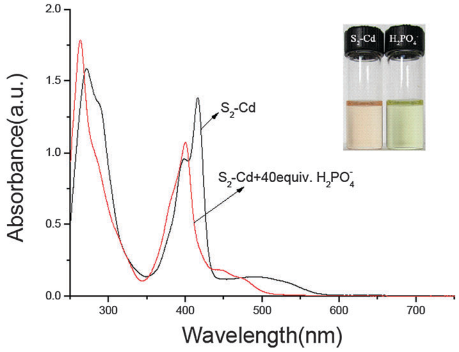

Fig. 4 Absorbance spectra of S_2–Cd (15 equiv.) in DMSO–H_2O (pH = 7.24, v/v = 8 : 2) in the presence of $H_2PO_4^-$ (40 equiv.). Inset: the photograph from left to right shows the change in the absorbance of S_2–Cd (15 equiv.), S_2–Cd (15 equiv.) + $H_2PO_4^-$ (40 equiv.) in DMSO–H_2O (pH = 7.24, v/v = 8 : 2).

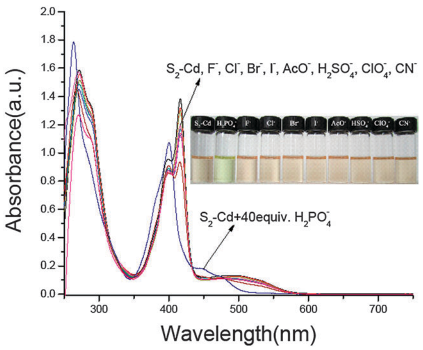

Fig. 5 Absorbance emission data for a mixture of S_2–Cd (15 equiv.) and each of the various anions as the tetrabutylammonium salts, in the DMSO–H_2O (pH = 7.24, v/v = 8 : 2) solution. Inset: color changes observed for S_2–Cd (15 equiv.) upon the addition of $H_2PO_4^-$, F^-, Cl^-, Br^-, I^-, AcO^-, HSO_4^-, ClO_4^-, CN^- (40 equiv., respectively) in DMSO–H_2O (pH = 7.24, v/v = 8 : 2).

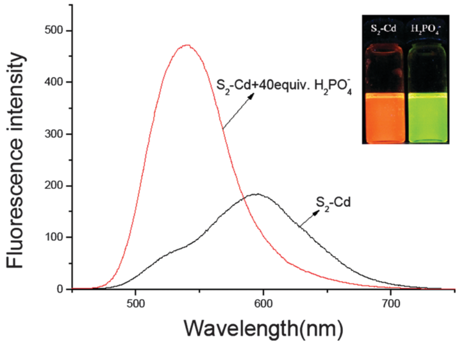

Fig. 6 Fluorescence spectra of S_2–Cd (15 equiv.) upon an excitation at 400 nm in DMSO–H_2O (pH = 7.24, v/v = 8 : 2) in the presence of $H_2PO_4^-$ (40 equiv.). Inset: the photograph from left to right shows the change in the fluorescence of S_2–Cd (15 equiv.), S_2–Cd + $H_2PO_4^-$ (40 equiv.) in DMSO–H_2O (pH = 7.24, v/v = 8 : 2).

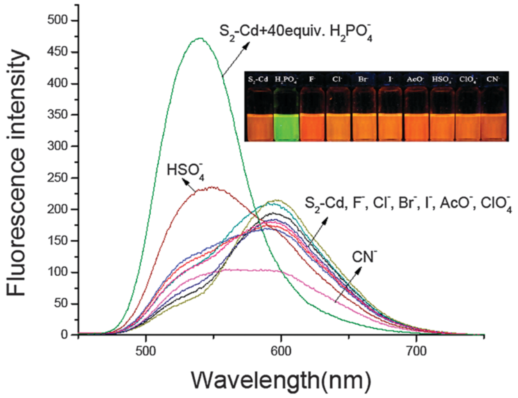

Fig. 7 Fluorescence emission data for a mixture of S_2–Cd and each of the various anions, as the tetrabutylammonium salts, in the DMSO–H_2O (pH = 7.24, v/v = 8 : 2) solution (excitation wavelength = 400 nm). Inset: visual fluorescence emissions of S_2–Cd (26.5 μM) upon the addition of $H_2PO_4^-$, F^-, Cl^-, Br^-, I^-, AcO^-, HSO_4^-, ClO_4^-, CN^- (40 equiv., respectively) in DMSO–H_2O (pH = 7.24, v/v = 8 : 2) on excitation at 365 nm using a UV lamp at rt.

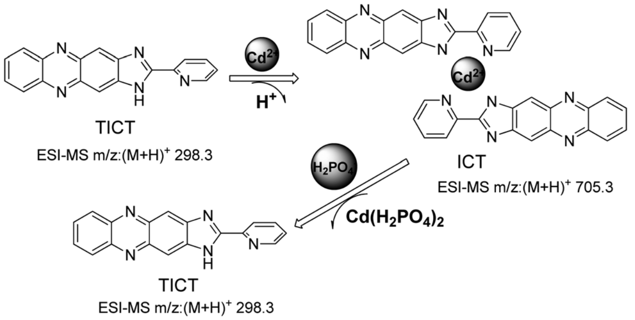

Fig. 8 The proposed structures of S_2 for Cd^{2+} and S_2–Cd for $H_2PO_4^-$ anions.

sensor S_2–Cd (15 equiv.), the same tests were also applied using F^-, Cl^-, Br^-, I^-, AcO^-, HSO_4^-, ClO_4^-, CN^- anions, and these anions induced little changes in the fluorescent spectrum of the sensor (Fig. 7).

As shown in Fig. 8, between the pyridine and phenazine units, there was a dihedral angle in S_2.[11,19] DFT studies agree with the evidence (ESI,†Fig. S8). Thus, the TICT states of the rotors caused the yellow emission of S_2. Upon the addition of Cd^{2+}, the interaction between Cd^{2+} and S_2 decreased the twisted intramolecular charge transfer ability and the formation of the S_2–Cd complex decreased the dihedral angle between the two units, further decreasing their electron transfer.[20,21] Thus, the binding of Cd^{2+} prohibited the TICT formation of S_2 and can enhance the coplanarity of the conjugated system[22] (ESI,† Fig. S8), largely promoting the strong red fluorescence emission. And upon the addition of $H_2PO_4^-$ to the S_2–Cd system, because of the interactions between $H_2PO_4^-$ and Cd^{2+}, the S_2–Cd complex was decomposed and the pyridine and phenazine units were nearly perpendicular *via* the conformational change. Thus, the binding of $H_2PO_4^-$ prohibited the ICT formation of free S_2 and can decrease the coplanarity of the conjugated system, largely promoting the yellow fluorescence emission.

The interaction and binding behavior between S_2–Cd (15 equiv.) and $H_2PO_4^-$ were investigated with their ^1H NMR, IR spectra and ESI-MS spectrum. As shown in Fig. 9, after adding 0.1–0.5 equiv. of Cd^{2+}, the NH (H_a) peak at 13.57 ppm disappeared. Meanwhile, the signal of the hydrogen atoms in the benzene and pyridine rings (8.87 ppm and 8.54 ppm) showed a downfield shift, indicating a charge transfer from the phenazine and pyridine groups to the Cd^{2+} ion.[23] However,

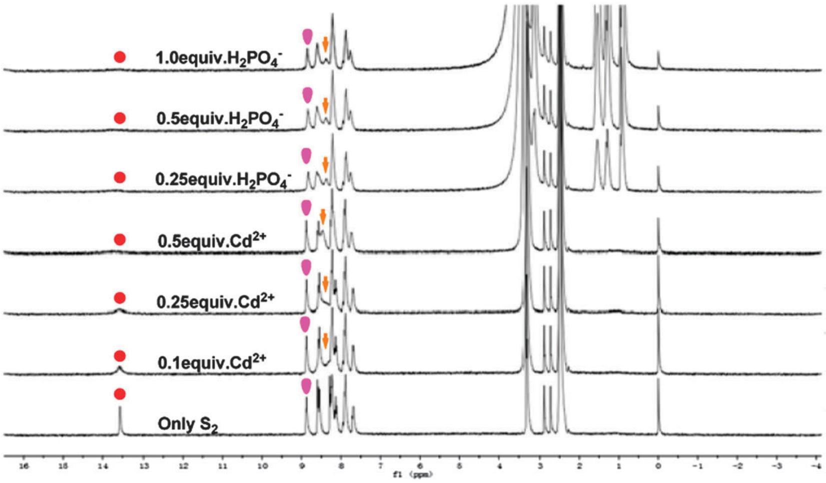

Fig. 9 ^{1}H NMR spectra (400 MHz, DMSO-d_6) of free S_2 and in the presence of Cd^{2+}, $H_2PO_4^-$, respectively.

as increasing concentrations of $TBAH_2PO_4$ were added to the solution of S_2–Cd, it was noted that the signal of the hydrogen atoms in the benzene and pyridine rings (8.76 ppm and 8.46 ppm) showed an upfield shift. Thus, the results of the ^{1}H NMR titration suggested that the conformational change between the phenazine and pyridine was attained during the ion recognition process. To elucidate the binding mode of S_2 with cadmium perchlorate, the IR spectrum of the S_2–Cd complex was recorded (ESI,† Fig. S5). The important change was observed in the absorption band corresponding to the C=N group in the imidazole ring, which shifts from 1658.68 to 1619.83 cm^{-1}. And the absorption band of NH at 3137.21 disappeared. In order to explore the interaction and binding mechanism of the present system, the products S_2 with Cd^{2+} and S_2–Cd with $H_2PO_4^-$ were subjected to mass spectral analyses. The ion peaks were detected at *m*/*z* 705.3 (ESI,† Fig. S6), which correspond to $[S_2–Cd–H]^+$. The peak at *m*/*z* 298.3 demonstrated the presence of $[M + H]^+$ (ESI,† Fig. S7). The M was indicated S_2 as a final product after $TBAH_2PO_4$ was added to the solution of S_2–Cd. Based on the above findings, we propose that the reaction mechanism in this system may proceed through the route depicted in Fig. 8: the presence of Cd^{2+} leads to the formation of S_2–Cd, which is then converted to a conformational change, producing the MS signals at *m*/*z* 705.3. After $TBAH_2PO_4$ was added to the solution of S_2–Cd, the S_2–Cd complex was decomposed and inorganic cadmium phosphate was formed.[24]

In addition, the interaction and binding mechanism were further confirmed by the UV-vis spectroscopy and Fluorescence spectroscopy. When 40 equivalents of $H_2PO_4^-$ were added to the DMSO–H_2O (8 : 2, v/v) HEPES buffer (pH 7.24) solutions of sensor S_2–Cd (15 equiv.), the optical absorbance and fluorescence intensity returned to the levels observed for the free compound S_2 (Fig. 10).

To further investigate the interaction between S_2–Cd (15 equiv.) and $H_2PO_4^-$, UV-vis absorption spectral variation of the sensor S_2–Cd (15 equiv.) in DMSO–H_2O (8 : 2, v/v) HEPES buffer (pH 7.24) was monitored during titration with different concentrations of $H_2PO_4^-$ from 0 to 14.59 equivalents. As shown in Fig. 11, seven isosbestic points are clearly observed at 268, 311, 328, 351, 405, 432 and 475 nm with increasing concentrations of $H_2PO_4^-$.

At the same time, fluorescence emission spectral variation of sensor S_2–Cd (15 equiv.) in DMSO–H_2O (8 : 2, v/v) HEPES buffer (pH 7.24) was monitored during titration with different concentrations of $H_2PO_4^-$ from 0 to 16.31 equivalents, as shown in Fig. 12. The selectivity of S_2–Cd (15 equiv.) for

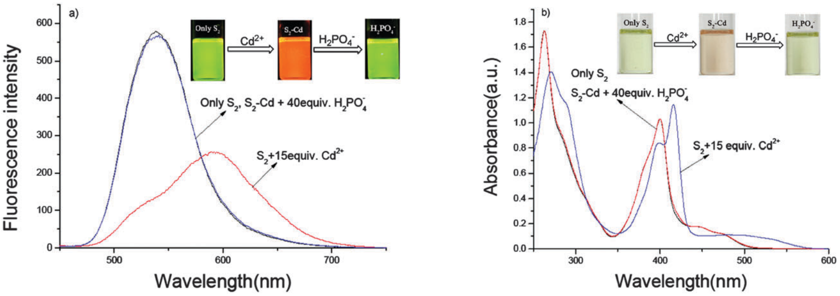

Fig. 10 (a) Fluorescence spectra of S_2, S_2–Cd (15 equiv.) and S_2–Cd + $H_2PO_4^-$ (40 equiv.) upon excitation at 400 nm in DMSO–H_2O (pH = 7.24, v/v = 8 : 2). Inset: the photograph from left to right shows the change in the fluorescence of S_2, S_2–Cd (15 equiv.), S_2–Cd + $H_2PO_4^-$ (40 equiv.) in DMSO–H_2O (pH = 7.24, v/v = 8 : 2). (b) Absorbance spectra of S_2, S_2–Cd (15 equiv.) and S_2–Cd + $H_2PO_4^-$ (40 equiv.) in DMSO–H_2O (pH = 7.24, v/v = 8 : 2). Inset: the photograph from left to right shows the color change in S_2, S_2–Cd (15 equiv.), S_2–Cd + $H_2PO_4^-$ (40 equiv.) in DMSO–H_2O (pH = 7.24, v/v = 8 : 2).

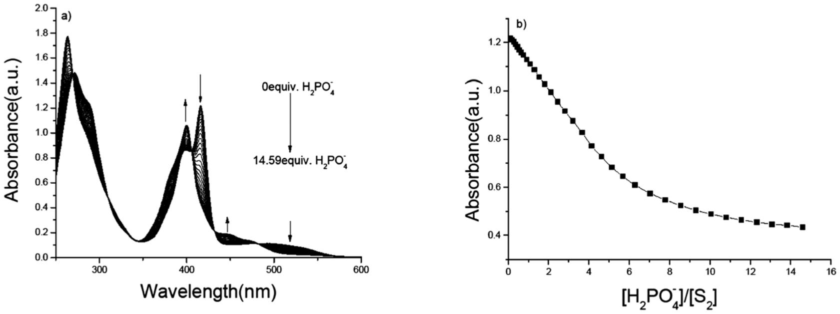

Fig. 11 (a) Absorbance spectra of S_2–Cd (15 equiv.) at different concentrations of $H_2PO_4^-$ (0-14.59 equiv.) in DMSO–H_2O (pH = 7.24, v/v = 8 : 2). (b) A plot of absorbance depending on the concentration of $H_2PO_4^-$ in the range from 0 to 14.59 equivalents. The detection wavelength was 400 nm.

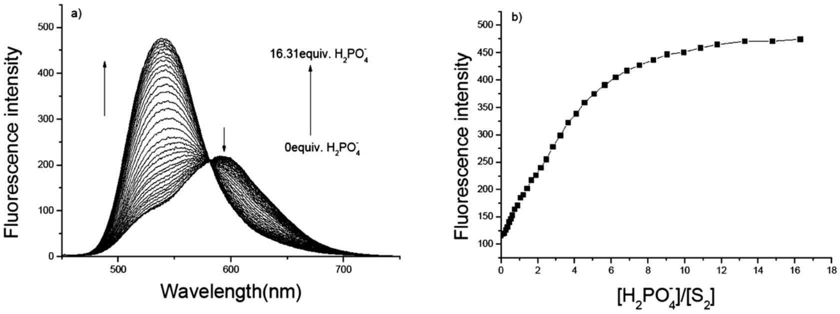

Fig. 12 (a) Fluorescence spectra of S_2–Cd (15 equiv.) at different concentrations of $H_2PO_4^-$ in DMSO–H_2O (pH = 7.24, v/v = 8 : 2). (b) A plot of fluorescence intensity depending on the concentration of $H_2PO_4^-$ in the range from 0 to 16.31 equivalents. The detection wavelength was 540 nm.

$H_2PO_4^-$ over other anions has been examined. Results of our studies have revealed that when 40 equivalents of other anions were added to the DMSO–H_2O (8 : 2, v/v) HEPES buffer (pH 7.24) solutions of S_2–Cd and $H_2PO_4^-$, all potentially competitive anions exerted no or little influence on the absorbance and fluorescence detection of $H_2PO_4^-$ in DMSO–H_2O (8 : 2, v/v) HEPES buffer (pH 7.24), as shown in Fig. 13.

To further validate the selectivity of S_2–Cd (15 equiv.) for $H_2PO_4^-$ over other metal ions, the same tests were also applied using Ca^{2+}, Cu^{2+}, Pd^{2+}, Zn^{2+}, Cr^{3+}, Mg^{2+} ions, Results of our studies have revealed that when 40 equivalents of other metal ions were added to the DMSO–H_2O (8 : 2, v/v) HEPES buffer (pH 7.24) solutions of S_2–Cd and $H_2PO_4^-$, these ions exerted no or little influence on the absorbance and fluorescence detection of $H_2PO_4^-$ in DMSO–H_2O (8 : 2, v/v) HEPES buffer (pH 7.24) except the Cu^{2+} ions (ESI,† Fig. S9).

The Job plot between S_2–Cd (15 equiv.) and $H_2PO_4^-$ was implemented, demonstrating a 1/2 stoichiometry for the

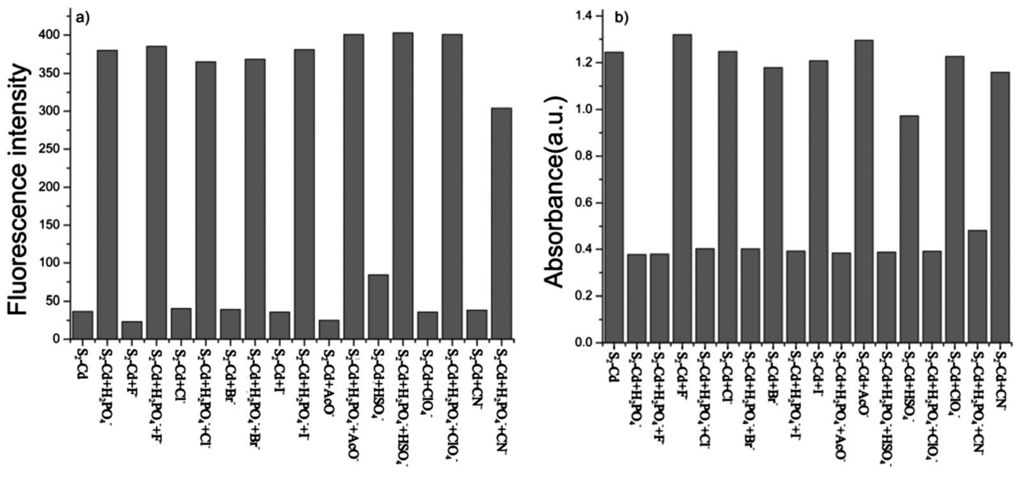

Fig. 13 (a) Fluorescence spectra of S_2–Cd (15 equiv.) in response to $H_2PO_4^-$ (40 equiv.) in the presence of various anion species in DMSO–H_2O (pH = 7.24, v/v = 8 : 2). The detection wavelength was 540 nm. (b) Absorbance spectra of S_2–Cd (15 equiv.) in response to $H_2PO_4^-$ (40 equiv.) in the presence of various anion species in DMSO–H_2O (pH = 7.24, v/v = 8 : 2). The detection wavelength was 416 nm.

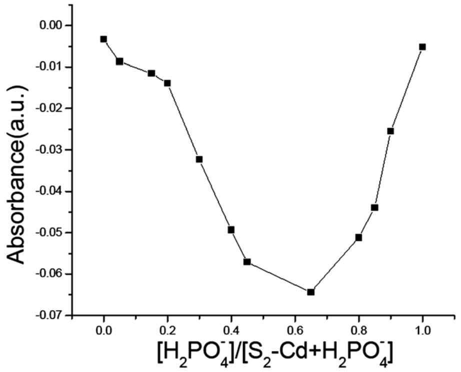

Fig. 14 Job's plot examined between $H_2PO_4^-$ and S_2–Cd, indicating the 1 : 2 stoichiometry clearly.

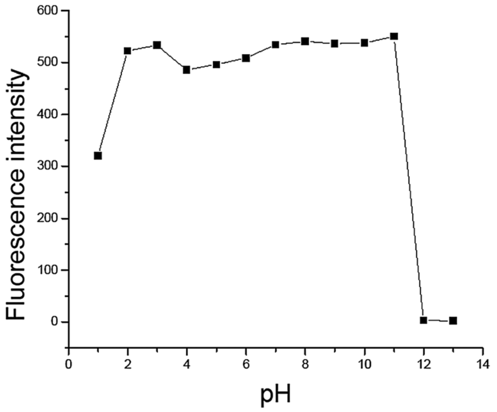

Fig. 15 Influence of pH on the fluorescence of S_2–Cd–$H_2PO_4^-$ in DMSO–H_2O (pH = 7.24, v/v = 8 : 2). Excitation wavelength is 400 nm.

S_2–Cd and $H_2PO_4^-$, as shown in Fig. 14. The association constant was determined to be 4.15×10^8 M^{-2} (ESI,† Fig. S4) and the detection limit of the sensor towards $H_2PO_4^-$ is 2.8×10^{-6} M, which indicates that this sensor could potentially be used as a probe for $H_2PO_4^-$ monitoring.

The selectivity of S_2–Cd (15 equiv.) to $H_2PO_4^-$ was examined over a wide range of pH values (Fig. 15). No apparent changes in the fluorescence spectra were observed, and the detection of $H_2PO_4^-$ can work well in the range of pH 2.0–11.0. To investigate the practical application of the sensor S_2–Cd, test trips were prepared by immersing a filter paper into a DMSO solution of S_2–Cd (0.1 M). The test strips containing S_2–Cd were utilized to sense $H_2PO_4^-$ and other anions. As shown in Fig. 16, when $H_2PO_4^-$ and the other anions were added on the test kits respectively, the obvious color change was observed only with $H_2PO_4^-$ solution under the 365 nm UV lamp. And potentially competitive anions exerted no influence on the detection of $H_2PO_4^-$ by the test strips. Therefore, the test strips could conveniently detect $H_2PO_4^-$ in solutions.

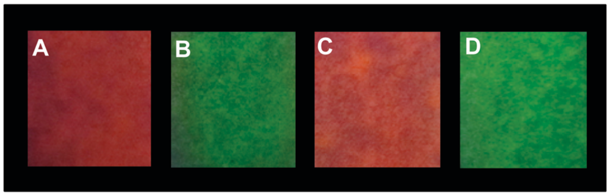

Fig. 16 Photographs of S_2–Cd on test papers (A) only S_2–Cd, (B) after immersion into DMSO–H_2O (pH = 7.24, v/v = 8 : 2) solutions with $H_2PO_4^-$, (C) after immersion into DMSO–H_2O (pH = 7.24, v/v = 8 : 2) solutions with others ions, (D) after immersion into DMSO–H_2O (pH = 7.24, v/v = 8 : 2) solutions with $H_2PO_4^-$ and other ions under irradiation at 365 nm.

4. Conclusion

In conclusion, we have presented a new long wavelength emission dihydrogen phosphate chemosensor (S_2–Cd) according to the twisted intramolecular charge transfer (TICT) mechanism based on the 2-pyridine-1*H*-imidazo[4,5-*b*]phenazine and Cd^{2+} complex. The sensor S_2–Cd showed both fluorescent and colorimetric selectivity for $H_2PO_4^-$ in DMSO–H_2O (8 : 2, v/v) HEPES buffer solutions. To the best of our knowledge, this is the first time that a long wavelength emission fluorescent chemosensor with high selectivity for $H_2PO_4^-$ was designed based on the 2-pyridine-1*H*-imidazo[4,5-*b*]phenazine and Cd^{2+} complex. Thus, it is believed that this receptor will have a role to play in the sensing, detection, and recognition of $H_2PO_4^-$ ions. In addition, test strips based on S_2–Cd were fabricated, which also exhibit a good selectivity to $H_2PO_4^-$ as in solution. We believe the test strips could act as convenient and efficient $H_2PO_4^-$ test kits.

Acknowledgements

This work was supported by the National Natural Science Foundation of China (No. 21064006, 21262032 and 21161018), the Program for Changjiang Scholars and Innovative Research Team in the University of Ministry of Education of China (No. IRT1177), the Natural Science Foundation of Gansu Province (No. 1010RJZA018), the Youth Foundation of Gansu Province (No. 2011GS04735) and NWNU-LKQN-11-32. We thank Dr Ran Fang (Lanzhou University) for DFT studies. The high performance computing facility at the Gansu Computing Center is also acknowledged.

References

1 D. H. Lee, S. Y. Kim and J. Hong, *Angew. Chem., Int. Ed.*, 2004, **43**, 4777.
2 J. R. Jadhav, M. W. Ahmad and H. S. Kim, *Tetrahedron Lett.*, 2012, **53**, 2627.
3 X. L. Ni, X. Zeng, C. Redshaw and T. Yamato, *J. Org. Chem.*, 2011, **76**, 5696.
4 S. L. Tobey and E. V. Anslyn, *Org. Lett.*, 2003, **5**, 2029.
5 V. Bhalla, V. Vij, M. Kumar, P. R. Sharma and T. Kaur, *Org. Lett.*, 2012, **14**, 1012.
6 A. Coskun, M. D. Yilmaz and E. U. Akkaya, *Org. Lett.*, 2007, **9**, 607.
7 Z. Guo, W. Zhu, M. Zhu, X. Wu and H. Tian, *Chem.–Eur. J.*, 2010, **16**, 14424.

8 C. H. Hung, G. F. Chang, A. Kumar, G. F. Lin, L. Y. Luo, W. M. Ching and E. G. Diau, *Chem. Commun.*, 2008, 978.

9 S. Atilgan, T. Ozdemir and E. U. Akkaya, *Org. Lett.*, 2008, **10**, 4065.

10 E. Lippert, W. LÜder, F. Moll, H. Nagele, H. Boos and H. Prigge, *Angew. Chem.*, 1961, **73**, 695.

11 G. Li, Y. C. Wu, J. K. Gao, C. Y. Wang, J. B. Li, H. C. Zhang, Y. Zhao, Y. L. Zhao and Q. C. Zhang, *J. Am. Chem. Soc.*, 2012, **134**, 20298.

12 A. B. Korzhenevskii, L. V. Markova, S. V. Efimova, O. I. Koifman and E. V. Krylova, *Russ. J. Gen. Chem.*, 2005, **75**, 980.

13 A. M. Amerl, A. A. E. Bahnasawil, M. R. H. Mahran and M. Lapib, *Monatshefte fÜr Chemie*, 1999, **130**, 1217.

14 A. A. E. Bahnasawy and M. F. E. Ahwany, *Phosphorus, Sulfur Silicon Relat. Elem.*, 2007, **8**, 1937.

15 Y. M. Zhang, Q. Lin, T. B. Wei, X. P. Qin and Y. Li, *Chem. Commun.*, 2009, 6074.

16 Y. M. Zhang, Q. Lin, T. B. Wei, D. D. Wang, H. Yao and Y. L. Wang, *Sens. Actuators, B*, 2009, **137**, 447.

17 Q. Lin, P. Chen, J. Liu, Y. P. Fu, Y. M. Zhang and T. B. Wei, *Dyes Pigm.*, 2013, **98**, 100.

18 T. B. Wei, P. Zhang, B. B. Shi, P. Chen, Q. Lin, J. Liu and Y. M. Zhang, *Dyes Pigm.*, 2013, **97**, 297.

19 L. P. Yang, J. R. Li, H. X. Chai, H. Y. Lu, Q. Zhang and D. X. Shi, *Chin. J. Chem.*, 2013, **31**, 443.

20 Y. Zhou, Z. X. Li, S. Q. Zang, Y. Y. Zhu, H. Y. Zhang, H. W. Hou and T. C. W. Mak, *Org. Lett.*, 2012, **14**, 1214.

21 Q. Q. Li, M. Peng, H. Y. Li, C. Zhong, L. Zhang, X. H. Cheng, X. N. Peng, Q. Q. Wang, J. G. Qin and Z. Li, *Org. Lett.*, 2012, **14**, 2094.

22 M. Suresh, A. K. Mandal, S. Saha, E. Suresh, A. Mandoli, R. D. Liddo, P. P. Parnigotto and A. Das, *Org. Lett.*, 2010, **12**, 5406.

23 J. Liu, M. Yu, X. C. Wang and Z. Zhang, *Spectrochim. Acta, Part A*, 2012, **93**, 245.

24 H. C. Visser, D. M. R. Kevich, W. V. Boom, F. K. D. Jong and D. N. R. Houdt, *J. Am. Chem. Soc.*, 1994, **116**, 11554.